

## PILLARED CLAYS PREPARED FROM THE REACTION OF CHROMIUM ACETATE WITH MONTMORILLONITE

ANTONIO JIMENEZ-LOPEZ, JOSE MAZA-RODRIGUEZ, PASCUAL OLIVERA-PASTOR,  
PEDRO MAIRELES-TORRES AND ENRIQUE RODRIGUEZ-CASTELLON

Departamento de Química Inorgánica Cristalografía y Mineralogía, Facultad de Ciencias  
Universidad de Málaga, Apartado 59, 29071-Málaga, España

**Abstract**—Refluxing chromium (III) acetate with a Na<sup>+</sup>-montmorillonite suspension gives rise to the intercalation of linear Cr(III) polyhydroxo-acetate oligomers. Thermally stable chromia pillared montmorillonite materials are obtained upon calcination under ammonia up to 625°C, and basal expansions up to 6 Å are maintained. The porous materials retain high surface areas (366–464 m<sup>2</sup> g<sup>-1</sup>), a micropore volume of 0.1 cm<sup>3</sup> g<sup>-1</sup> and narrow pore size distributions centered between 7.5 and 12 Å. The most thermally stable materials in air were those prepared under ammonia at 625°C, containing NH<sub>4</sub><sup>+</sup> as the exchangeable ion.

**Key Words**—Chromia, Montmorillonite, Pillaring.

### INTRODUCTION

Pillared layered compounds are porous, thermally stable materials with attractive catalytic properties (Mitchell, 1990). In particular, smectite clays pillared by metal oxides have been used successfully as acid catalysts in several organic reactions (Adams, 1987). Chromia pillared materials are of particular interest because the interlayer pillaring agent itself is catalytically active.

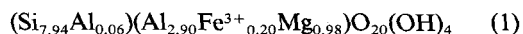
Various polycationic species of Cr(III) have been intercalated in clays (Brindley and Yamanaka, 1979; Carr, 1985; Pinnavaia *et al.*, 1985) leading to a variety of materials with high basal expansions and specific surface areas. The type of polynuclear metal unit intercalated in the interlayers determines the characteristics of the pillared materials—i.e., surface area, porosity, and acidity—and, hence, the catalytic properties. Recently, the oligomeric chromium species from solutions of chromium nitrate partially hydrolyzed with Na<sub>2</sub>CO<sub>3</sub> at 95°C (Pinnavaia *et al.*, 1985; Tzou and Pinnavaia, 1988) have been identified via EXAFS studies (Bornholdt *et al.*, 1991). For a CO<sub>3</sub><sup>2-</sup>/Cr<sup>3+</sup> molar ratio 0.5, the pillaring solution contains tetranuclear species with *cis*-linked edge-bridged octahedral units, which are retained on incorporation into montmorillonite. The catalytic activity of some chromia pillared clays prepared using these pillaring solutions has been reported (Pinnavaia *et al.*, 1985; Tzou and Pinnavaia, 1988).

In previous work, we reported the preparation and characterization of porous chromia pillared layered phosphates obtained from the reaction of Cr(CH<sub>3</sub>CO<sub>2</sub>)<sub>3</sub> (Cr(OAc)<sub>3</sub>) with colloidal layered phosphates (Maireles-Torres *et al.*, 1991a, 1991b). The resulting intercalation compounds, with well defined Cr<sup>3+</sup>-polyhydroxyacetato species inserted within the phosphate

matrix, leads to a series of chromia pillared materials with basal expansions of 5–20.5 Å and surface areas of 250–330 m<sup>2</sup> g<sup>-1</sup>, after calcination under N<sub>2</sub>. This procedure provides a buffered medium (pH = 4) without any competitive cation in solution, permitting *in situ* growth of linear oligomeric chromium species on the host surface. The acidity of layered phosphates is strongly increased by the incorporation of chromia pillars, which catalyze the dehydration of isopropyl alcohol. In addition, selectivity can be controlled according to the chromium content (Guerrero-Ruiz *et al.*, 1992). This method is now extended to a smectite clay (montmorillonite) with the objective of obtaining new acid porous materials with potential catalytic uses.

### EXPERIMENTAL METHODS

The montmorillonite used came from Tidinit, Morocco. A Na<sup>+</sup>-exchanged sample with particle size < 2 μm was used as the starting material. The structural formula calculated from the chemical analysis is



and the cation exchange capacity (CEC) is 1.25 meq/g, based on the weight of the sample heated at 900°C.

An aqueous suspension of 1 g of Na<sup>+</sup>-montmorillonite was contacted with increasing quantities of Cr(OAc)<sub>3</sub>, varying the Cr<sup>3+</sup> concentrations from 9–366 mmol/dm<sup>3</sup> (final volume, 200 ml). In other series of experiments, the final volume was reduced to 100 ml in order to study the effect of the chromium concentration in solution for a given Cr<sup>3+</sup>/clay ratio. In all cases, each suspension was refluxed for 10 days, cooled, centrifuged, washed with deionized water to a conductance of washing waters < 40 μS, then air-dried, and analyzed (C, H, N, TG, Cr analyses).

XRD of cast films obtained by dropping and drying

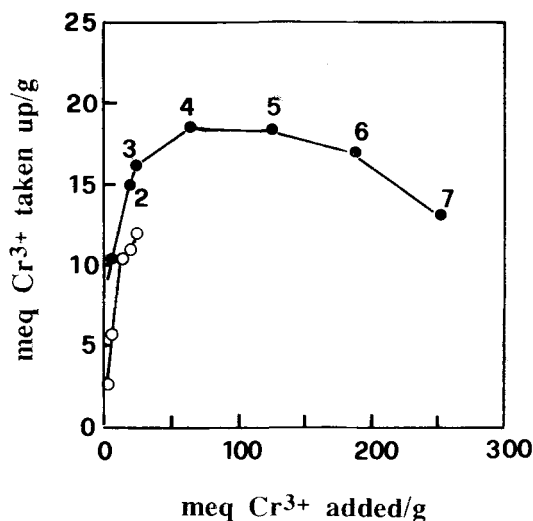


Figure 1. Uptake of hydrolyzed  $\text{Cr}(\text{OAc})_3$  species by  $\text{Na}^+$ -montmorillonite, (o) obtained using twice concentrated  $\text{Cr}^{3+}$  solutions at the same  $\text{Cr}/\text{clay}$  ratio.

the clay suspension on a glass slide were recorded on a Siemens D501 diffractometer ( $\text{CuK}\alpha$  radiation). TG and DTA were measured on a Rigaku Thermoflex instrument (calcined  $\text{Al}_2\text{O}_3$  as reference;  $10^\circ\text{C min}^{-1}$  heating rate).  $\text{Cr}^{3+}$  was analyzed colorimetrically using the chromate method ( $\lambda = 372 \text{ nm}$ ) on alkaline solutions after treatment with  $\text{NaOH-H}_2\text{O}_2$ . Optical spectra (diffuse reflectance) were registered on a Shimadzu MPC 3100 spectrophotometer ( $\text{BaSO}_4$  as reference) and IR spectra on a Perkin-Elmer 883 spectrophotometer as KBr disks. Adsorption-desorption of  $\text{N}_2$  was measured on a conventional volumetric apparatus ( $77\text{K}$ ; degassing at  $200^\circ\text{C}$ ;  $10^{-4}$  mbar overnight).

## RESULTS AND DISCUSSION

Previous studies have showed that polymeric species of  $\text{Cr}^{3+}$ -hydroxoacetate may be intercalated into layered phosphates by refluxing  $\text{Cr}(\text{OAc})_3$  aqueous solutions with colloidal suspensions of these ion exchangers. In most cases, the oligomeric chromium species intercalated were well-defined, single linear trinuclear, tetranuclear, pentanuclear or hexanuclear species (Maireles-Torres *et al.*, 1991a, 1991b).

The uptake of chromium acetate by montmorillonite occurs in a fashion similar to that in layered phosphates (Figure 1). Initially,  $\text{Cr}^{3+}$  uptake increases with increasing concentrations of  $\text{Cr}^{3+}$  in solution, but additions higher than 120 meq/g lead to materials with lower  $\text{Cr}^{3+}$  loadings. This uptake curve is typical for processes in which species association takes place in solution (Giles *et al.*, 1960). Thus, larger oligomers formed at high  $\text{Cr}^{3+}$  concentration are increasingly difficult to accommodate into the matrix. Montmorillonite takes up large amounts of  $\text{Cr}^{3+}$ , in excess of the

Table 1. Composition data of air-dried  $\text{Cr}^{3+}$ -polyhydroxoacetate montmorillonite intercalates.

Sample	$[\text{Cr}^{3+}]_{\text{add}}$ (mol liter $^{-1}$ )	meq. $\text{Cr}^{3+}$ add./g ( $900^\circ\text{C}$ )	meq. $\text{Cr}^{3+}$ taken up/g ( $900^\circ\text{C}$ )	% $\text{OAc}^-$	$\text{OAc}^-/\text{Cr}$ ratio	% $\text{H}_2\text{O}$
1	0.009	6.2	10.5	1.21	0.18	12.5
2	0.027	18.7	15.1	2.09	0.24	11.7
3	0.037	25.0	16.2	2.80	0.28	9.57
4	0.091	62.5	18.5	3.91	0.38	16.6
5	0.183	125.0	18.4	4.39	0.42	13.5
6	0.274	187.5	17.1	4.67	0.48	12.5
7	0.366	250.0	13.2	5.70	0.72	10.6

theoretical exchange capacity. This is attributable to the significant reduction of the charge per cation ratio in oligomeric species, the maximum uptake being 18.5 meq  $\text{Cr}^{3+}/\text{g}$  ( $900^\circ\text{C}$ ). When the concentration of  $\text{Cr}^{3+}$  is increased by reducing the final volume to 100 ml, intercalation compounds with lower  $\text{Cr}^{3+}$  loadings are obtained (Figure 1). Table 1 lists the chemical analyses of  $\text{Cr}^{3+}$  exchanged montmorillonite samples. The  $\text{OAc}^-/\text{Cr}^{3+}$  ratio in these materials increases with the  $\text{Cr}^{3+}$  concentration in solution from 0.18 to 0.72; therefore, the oligomers intercalated in montmorillonite are polyhydroxy acetate  $\text{Cr}^{3+}$  moieties. In addition, the interlayer water contents are quite high.

Chemical compositions per unit cell  $[\text{O}_{20}(\text{OH})_4]$  are listed in Table 2. The Cr contents are in the range found by other authors (Brindley and Yamanaka, 1979; Tzou and Pinnavaia, 1988), but empirical formulae of single species, like those found for zirconium phosphate, cannot be established, suggesting the presence of more than one species in the interlayer region of montmorillonite. This agrees with broadening of bands in optical spectra and diffraction peaks in XRD patterns. The samples 2–7 present similar  $\text{Cr}^{3+}$  contents but different  $\text{Cr}/\text{OAc}$  ratios, water contents, and basal spacings, suggesting that the oligomeric species intercalated should possess different polymerization degree and charge. Polymerization increases with the concentration of  $\text{Cr}^{3+}$  in solution (Maireles-Torres *et al.*, 1991a, 1991b).

The diffuse reflectance spectra (Figure 2) are similar to those found for the chromium oligomers intercalated in  $\alpha$ -tin and  $\alpha$ -zirconium phosphates, i.e., they show

Table 2. Chemical composition per unit cell  $[\text{O}_{20}(\text{OH})_4]$  and  $d_{001}$  basal spacings of air-dried  $\text{Cr}^{3+}$ -polyhydroxoacetate montmorillonite intercalates.

Sample	Empirical formulation	$d_{001}$ ( $\text{\AA}$ )
1	$\text{Cr}_{2.41}(\text{OAc})_{0.45}(\text{OH})_{5.98}(\text{H}_2\text{O})_{6.25}\text{-Mont}$	16.5
2	$\text{Cr}_{3.46}(\text{OAc})_{0.83}(\text{OH})_{8.75}(\text{H}_2\text{O})_{6.16}\text{-Mont}$	18.9
3	$\text{Cr}_{3.74}(\text{OAc})_{1.04}(\text{OH})_{9.38}(\text{H}_2\text{O})_{4.76}\text{-Mont}$	20.4
4	$\text{Cr}_{4.26}(\text{OAc})_{1.50}(\text{OH})_{10.48}(\text{H}_2\text{O})_{9.22}\text{-Mont}$	17.7
5	$\text{Cr}_{4.24}(\text{OAc})_{1.68}(\text{OH})_{10.24}(\text{H}_2\text{O})_{7.42}\text{-Mont}$	17.1
6	$\text{Cr}_{3.94}(\text{OAc})_{1.79}(\text{OH})_{9.20}(\text{H}_2\text{O})_{6.75}\text{-Mont}$	16.4
7	$\text{Cr}_{3.04}(\text{OAc})_{2.18}(\text{OH})_{6.14}(\text{H}_2\text{O})_{5.42}\text{-Mont}$	16.3

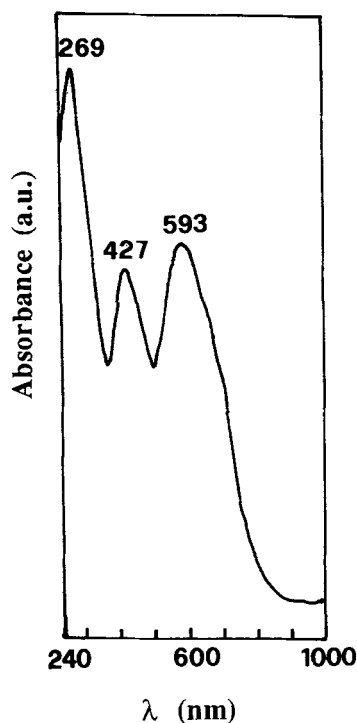


Figure 2. Optical spectrum of a  $\text{Cr}^{3+}$ -polyhydroxoacetate montmorillonite intercalate (Sample 2).

the  $4_{T_{2g}} \leftarrow 4_{A_{2g}}(\nu_1)$  and  $4_{T_{1g}} \leftarrow 4_{A_{2g}}(\nu_2)$  transitions typical of a six-coordinate geometry for  $\text{Cr}^{3+}$ . The intensity ratios of these absorption bands for all intercalates were in the range 1.07–1.26, suggesting the presence of linear oligomers of chromium in the interlayer space of the silicate (Maireles-Torres *et al.*, 1991a, 1991b). It seems that requirements of charge neutralization in the sterically restricted interlamellar region preclude the formation of compact structures, such as those believed to exist in compact (Monsted *et al.*, 1985).

The  $d_{001}$  basal spacings of the  $\text{Cr}^{3+}$ -polyhydroxyacetate intercalates (Table 2) vary between 16.3 and 20.4 Å. These values do not correlate with chromium and interlayer water contents, which can be attributed to different arrangements of  $\text{Cr}^{3+}$  oligomers in the interlayer region depending on their charges and sizes.  $\text{Cr}^{3+}$ -polyhydroxoacetate oligomers are intercalated into layered phosphates in a more ordered way (narrower diffraction peaks) with higher interlayer distances. It appears that short (i.e., those with lower charge) oligomers tend to orient perpendicular to the layer, whereas larger ones (i.e., those with higher charge) preferentially adopt a slanted position. Moreover, the phosphates, which have a very high charge density, can intercalate bilayers of these oligomers (Maireles-Torres *et al.*, 1991a, 1991b). The montmorillonite surface, which has a much lower charge density than those of layered phosphates, allows the oligomers to lie in a

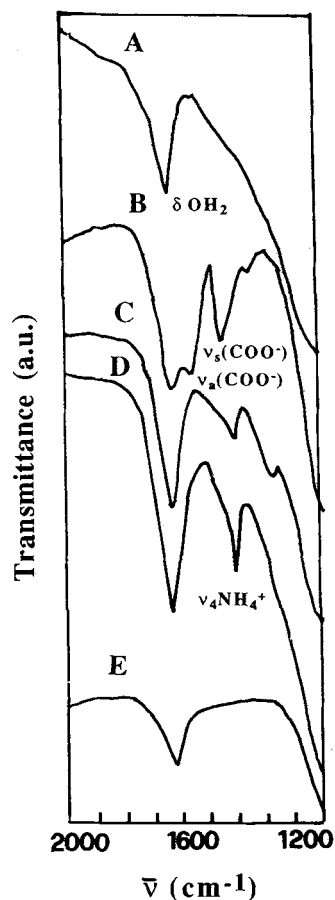


Figure 3. Infrared spectra of: (A)  $\text{Na}^+$ -montmorillonite; (B) material 3 freshly prepared; (C) material 3 calcined in  $\text{NH}_3$  at 400°C; (D) material 3 calcined in  $\text{NH}_3$  at 500°C; (E)  $\text{Na}^+$ -exchanged material (D).

more tilted position with respect to the layer; thus, materials with lower  $\text{Cr}^{3+}$  loadings are obtained. It is inferred, therefore, that the hydrolysis of  $\text{Cr}^{3+}$  is forced on the exchanger surface; thus, the products obtained depend on the surface characteristics. According to Tzou and Pinnavaia (1988), the X-ray basal spacing of the products depends on the extent of metal ion hydrolysis and the metal ion/clay ratio used in the pillaring reaction. For an optimum ratio of 50 mmol Cr added/meq clay, they reported basal spacings for air-dried samples between 16.3 and 27.6 Å corresponding to  $\text{CO}_3^{2-}/\text{Cr}^{3+}$  molar ratios between 0.0 and 1.25. The basal spacing values found here are similar to those reported by these authors for  $\text{CO}_3^{2-}/\text{Cr}^{3+} < 0.75$ . It is suggested that linear chromium oligomers, intercalated by *in situ* polymerization of  $\text{Cr}(\text{OAc})_3$  on the montmorillonite surface, gradually adopt a more slanted disposition as the polymerization degree and charge increase, i.e., as the  $\text{Cr}^{3+}$  concentration of the pillaring solution increases; the basal spacing of the intercalates thus decreases gradually for high chromium concen-

Table 3.  $d_{001}$  basal spacings of  $\text{Cr}^{3+}$ -exchanged montmorillonite materials calcined under ammonia at different temperatures.

Sample	$d_{001}$ (Å)		
	200°C	400°C	500°C
1	14.6	12.8	12.3
2	15.6	15.3	15.3
3	15.8	15.6	15.2
4	14.6	14.2	14.4
5	14.2	13.7	13.3
6	13.9	13.2	13.1
7	14.0	12.4	12.4

trations in solution. Conversely, oligomers prepared by partial hydrolysis of  $\text{Cr}(\text{NO}_3)_3$  with carbonate are presumably high connectivity rigid structures, which do not change on incorporation into the clay (Bornholdt *et al.*, 1991).

IR spectra of all products (Figure 3) show the characteristic bands of the  $\text{COO}^-$  group at 1550 and 1450  $\text{cm}^{-1}$ , corresponding to the asymmetrical ( $\nu_{\text{as}}$ ) and symmetrical ( $\nu_{\text{s}}$ ) stretching vibrations, respectively. The difference  $\nu_{\text{as}(\text{COO})} - \nu_{\text{s}(\text{COO})}$  is 100  $\text{cm}^{-1}$ , which is characteristic of the presence of bidentate  $\text{OAc}^-$  groups (Nakamoto, 1986). It has been suggested (Maireles-Torres *et al.*, 1991a, 1991b) that the presence of bidentate acetate ligands in intercalated  $\text{Cr}^{3+}$ -oligomers precludes formation of high connectivity clusters similar to those found in solution (Stunzi and Marty, 1983).

Calcination of these materials above 200°C in air or  $\text{N}_2$  leads to collapsed structures with segregation of chromium oxide; this is detected in the XRD patterns of the samples heated at  $T > 400^\circ\text{C}$  by the appearance of distinctive diffraction peaks at 3.6, 2.6 and 2.5 Å, which correspond to those of  $\text{Cr}_2\text{O}_3$  (Powder Diffraction File, 1967).

The mechanism that operates in the formation of these collapsed structures by calcination in air is a triple process of oxidation-segregation-reduction. Oxidation of  $\text{Cr}(\text{III})$  and organic matter occurs on calcination in air between 220° and 340°C (exothermic effect in DTA curves). The  $\text{CrO}_3$  formed is subsequently segregated from the interlayer region and then is reduced at higher temperatures. The presence of  $\text{Cr}(\text{VI})$  is detected by washing the samples calcined in air at 300°C: A yellow solution of  $\text{H}_2\text{Cr}_2\text{O}_7$  immediately forms. Formation of collapsed structures upon calcination in inert atmosphere was not expected to occur (Pinnavaia *et al.*, 1985; Maireles-Torres *et al.*, 1991a, 1991b); however, all materials calcined under  $\text{N}_2$  presented basal spacings lower than 10.5 Å. Although the mechanism is unclear, it is assumed that an abrupt release of protons is responsible for the segregation of chromium oxide from the interlayers. Protons can migrate toward the vacancies in the octahedral sites at high temperature, progressively reducing the negative charge of the montmorillonite layer (Poncelet and Schutz, 1986).

Table 4. Textural parameters for chromia-montmorillonite samples obtained under  $\text{NH}_3$  at 500°C.

Sample	$S_{\text{BET}}$	$C_{\text{BET}}$	$S_{\text{Lang}}$	$V_{\text{microp.}}^*$	$S_{\text{ext.}}^*$
1	274	596	366	0.10	51
2	333	401	424	0.12	120
3	353	567	464	0.14	79
4	349	541	446	0.14	121
5	344	533	390	0.11	85
6	328	535	391	0.12	81
7	291	557	388	0.12	70

\* Calculated by the  $\alpha$ -method.

Calcination under  $\text{NH}_3$  instead leads to a series of expanded materials stable up to 625°C, with still recognizable basal spacings in the range of 12.3–15.3 Å (Table 3) and high specific surface areas (Table 4). Ammonia retains the protons released during calcination (Vaughan, 1988), and the presence of  $\text{NH}_4^+$  ions stabilizes  $\text{Cr}(\text{III})$  because  $\text{NH}_4^+$  tends to reduce  $\text{Cr}(\text{VI})$  to  $\text{Cr}(\text{III})$  at high temperatures (Cotton and Wilkinson, 1988). Inasmuch as we have not detected the characteristic diffraction peaks of  $\text{Cr}_2\text{O}_3$  during calcination of the samples under  $\text{NH}_3$ , we have concluded that no chromium oxide is precipitated on the external surface of the mineral.  $\text{NH}_4^+$  ions are indicated in the interlayer region by the appearance of a new band in the IR spectra at 1400  $\text{cm}^{-1}$  (Figure 3) attributed to the

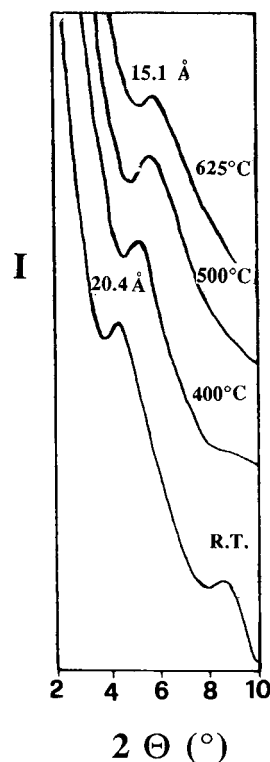


Figure 4. XRD patterns of material 3 freshly prepared and calcined in  $\text{NH}_3$  at different temperatures.

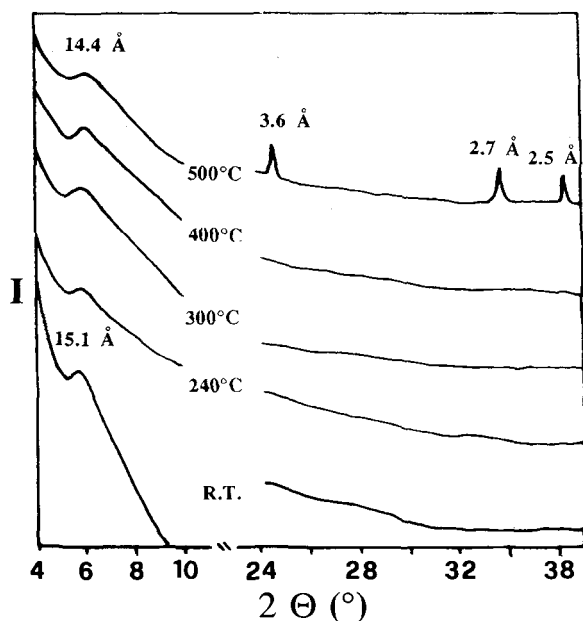


Figure 5. XRD patterns of material 3 prepared under  $\text{NH}_3$  at  $625^\circ\text{C}$  and then treated at different temperatures in air.

vibration mode  $\nu_4$ . This band disappears when the sample is treated with a 1 M NaCl solution (due to the replacement of  $\text{NH}_4^+$  by  $\text{Na}^+$ ).

The basal spacings of the samples calcined under  $\text{NH}_3$  decrease by between 2 and  $4.5 \text{ \AA}$  at  $200^\circ\text{C}$ , which is attributable to the loss of water with concomitant rearrangement of the oligomers in the interlayer space. Above this temperature, only a minor decrease is observed for Samples 2, 3, and 4, which retain basal spacing higher than  $14 \text{ \AA}$ , a threshold value for considering a layered structure to be pillared (Vaughan, 1988). The maximum basal expansion reached is about  $6 \text{ \AA}$ , assuming a layer thickness of  $9.5 \text{ \AA}$ , for Samples 2 and 3. The basal spacings of these materials calcined in  $\text{NH}_3$  at  $T > 400^\circ\text{C}$  did not change after treatment with diluted HCl solution or with  $\text{MCl}_n$  solution ( $\text{M}^{n+}$  = metal ion), confirming that a true pillaring of chromia nanostructures within the interlayer of montmorillonite has occurred. Ammonium exchanged chromia pillared montmorillonite (Sample 3) has a cation exchange capacity of  $0.34 \text{ meq/g}$ , and the  $\text{NH}_4^+$  ion is easily replaced by other metallic ions. Figure 4 shows the evolution of the  $d_{001}$  basal spacing of Sample 3 upon calcination under  $\text{NH}_3$ . Under these conditions the material is thermally stable up to  $625^\circ\text{C}$  and still maintains a basal expansion of  $5.7 \text{ \AA}$ .

The thermal stability of the pillared products prepared in  $\text{NH}_3$  atmosphere was tested by calcining these materials in air. The results obtained for Sample 3 are illustrated in Figure 5. The thermal stability of chromia pillared montmorillonite depends critically on the temperature at which the material was obtained under  $\text{NH}_3$ :

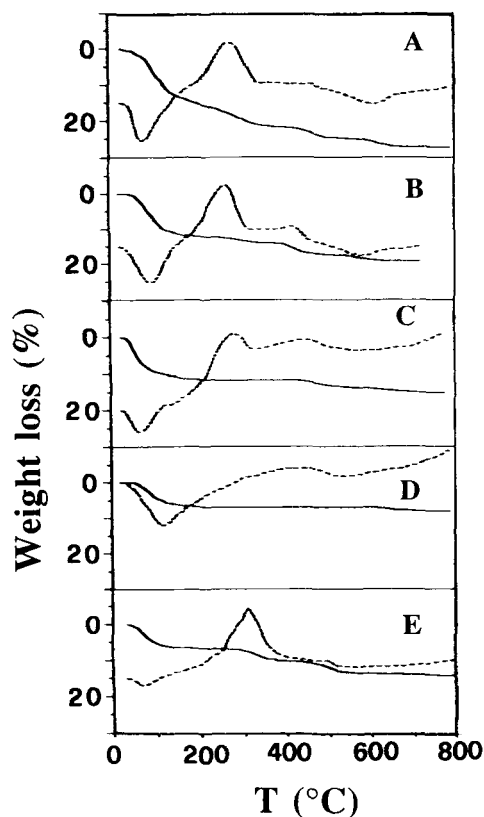
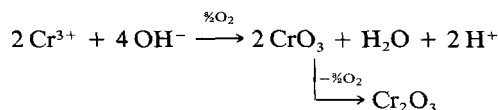


Figure 6. DTA-TG curves of material 3 at different conditions: (A) as prepared; (B) calcined in  $\text{NH}_3$  at  $400^\circ\text{C}$ ; (C) calcined in  $\text{NH}_3$  at  $500^\circ\text{C}$ ; (D) calcined in  $\text{NH}_3$  at  $600^\circ\text{C}$ ; (E)  $\text{Na}^+$ -exchanged material (C).

the higher the temperature, within the range  $400^\circ\text{--}625^\circ\text{C}$ , the higher the stability in air. Thus, the sample calcined under  $\text{NH}_3$  at  $625^\circ\text{C}$  is stable in air up to  $500^\circ\text{C}$ . Conversely, calcination below  $600^\circ\text{C}$  under  $\text{NH}_3$  leads to materials less stable in air, with partial segregation of chromium oxide at  $T > 300^\circ\text{C}$ ; and this result increases when the temperature of calcination in  $\text{NH}_3$  is decreased. The thermal stability of the pillared materials in air can also be appreciated by observing the corresponding TG-DTA curves (Figure 6). An exothermic effect centered at  $270^\circ\text{C}$  is apparent in DTA curves of the sample prepared at  $T < 600^\circ\text{C}$  while it is absent for the sample obtained at  $625^\circ\text{C}$ . The intensity of the exothermic effect increases when the preparation temperature under  $\text{NH}_3$  is decreased. This exothermic effect is associated with formation of  $\text{CrO}_3$ , which is segregated from the interlayer of montmorillonite and then reduced to  $\text{Cr}_2\text{O}_3$ , according to the reaction:



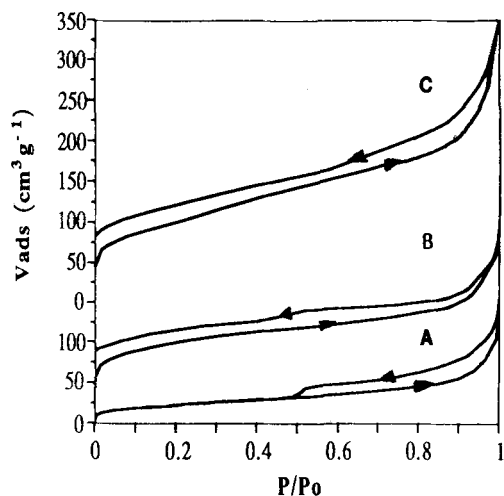


Figure 7. Adsorption-desorption isotherms of  $N_2$  at 77 K on: (A)  $Na^+$ -montmorillonite; (B) material 3 calcined in  $NH_3$  at 500°C; (C) material 4 calcined in  $NH_3$  at 500°C.

although mixed-oxidation species, including Cr(IV) and Cr(V) may also be formed (Maireles-Torres *et al.*, 1991a, 1991b).

The  $OH^-$  groups must be involved in the oxidation process inasmuch as higher calcination temperatures under  $NH_3$  (i.e., lower  $OH^-$  content) lead to less extensive oxidation. The weight loss of pillared materials between 270–400°C, attributed to the removal of water, decreases when the calcination temperature under  $NH_3$  increases from 400° to 625°C.

Oxidation of intercalated Cr(III)-oligomers occurred at higher temperature than that observed for chromia gels (Navarro-Martos, 1977) because of protection by the silicate matrix. Inversely, the structure of montmorillonite is stabilized by the presence of  $Cr_2O_3$  pillars; thus, the possibility of condensation of structural  $OH^-$  groups is reduced: Only a slight weight loss is observed at  $T > 600^\circ C$ , whereas the original Na-montmorillonite starts to lose structural water at 550°C. If the interlayer  $NH_4^+$  ion is replaced by other ions, e.g.,  $Na^+$ , the extent of oxidation of the interlayer Cr(III) increases (Figures 6C and 6E).

The adsorption-desorption isotherms of  $N_2$  at 77 K were measured on the sodium-montmorillonite samples at 200°C and on chromia montmorillonite samples prepared under  $NH_3$  at 500°C. As shown in Figure 7, insertion of  $Cr_2O_3$  in the interlayer of montmorillonite causes noticeable changes on the silicate surface. The isotherms of the pillared samples are characteristic of microporous solids, but with a contribution of mesopores (Gregg and Sing, 1982), which is more evident in the samples with lower basal spacings. The microporous nature of the samples is confirmed by the high values of the  $C_{BET}$  parameter (Table 4) and the existence of low pressure hysteresis, as is characteristic of

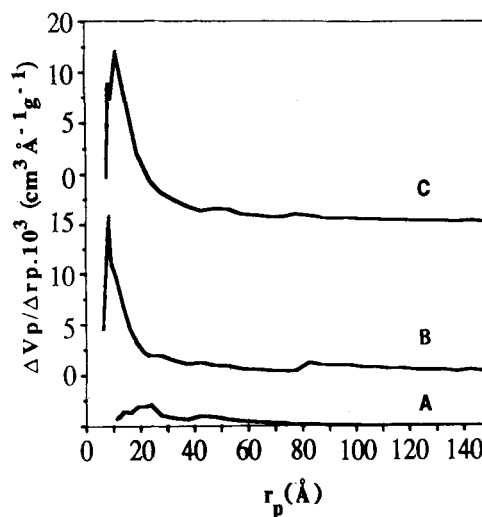


Figure 8. Pore size distributions of: (A)  $Na^+$ -montmorillonite; (B) material 3 calcined in  $NH_3$  at 500°C; (C) material 4 calcined in  $NH_3$  at 500°C.

ultramicrospheres, i.e., pores with sizes between 3 and 7 Å (Gregg and Sing, 1982). The isotherm corresponding to the original sample is of type IV, characteristic of a mesoporous material.

The values of the specific surface areas (Langmuir and BET),  $C_{BET}$  parameters, micropore volumes, and external surfaces are listed in Table 4. The micropore volumes and external surfaces were calculated by the  $\alpha$ -method, using a hydroxylated silica as standard (Gregg and Sing, 1982). Similar values of micropore volumes are obtained by the Dubinin method (Dubinin, 1966).

The specific surface areas of the chromia-montmorillonite samples are increased substantially with respect to the Na-montmorillonite (62  $m^2/g$ ). Since the external surfaces are of the order of the initial clay, it is inferred that the increase in the specific surface area of chromia-montmorillonite samples is due to the presence of micropores created by chromia pillars in the interlayer region. Although the basal spacings of these chromia-pillared materials are lower than those reported by Pinnavaia *et al.* (1985), the specific surface areas are quite similar.

The micropore volume values are of the order of 0.12  $cm^3/g$ , which are close to those of other pillared montmorillonites (Pesquera *et al.*, 1991).

Pore size distributions, determined by the Cranston method (Cranston and Inkley, 1957), are shown in Figure 8. The majority of pores in chromia-montmorillonite samples are in a narrow radius range between 7.5 and 20 Å, which supports the presence of a true pillaring model. Pore size distribution is more dependent on the type of  $Cr^{3+}$ -oligomer intercalated than on the interlayer distance of the calcined product.

## ACKNOWLEDGMENTS

The authors thank the CICYT (Spain) Project no. MAT 90-298 for financial support.

## REFERENCES

- Adams, J. M. (1987) Synthetic organic chemistry using pillared cation-exchange acid-treated montmorillonite catalyst. A review: *App. Clay Sci.* **2**, 309-342.
- Bornholdt, K., Corker, J. M., Evans, J., and Rummey, J. M. (1991) EXAFS Studies of the Formation of Chromia Pillared Clay Catalysts: *Inorg. Chem.* **30**, 2-4.
- Brindley, G. W. and Yamanaka, S. (1979) A study of hydroxychromium montmorillonites and the form of the hydroxychromium polymers: *Amer. Mineral.* **64**, 830-835.
- Carr, R. M. (1985) Hydration states of interlaminal chromium ions in montmorillonite: *Clays & Clay Minerals* **3**, 357-361.
- Cotton, F. A. and Wilkinson, G. (1988) *Advanced Inorganic Chemistry*, 5th ed., Wiley, New York.
- Cranston, R. W. and Inkley, F. A. (1957) The determination of pore structures from nitrogen adsorption isotherms: *Adv. Catal.* **9**, 143-156.
- Dubinin, M. M. (1966) *Chemistry and Physics of Carbon*, P. L. Walker, ed., Vol. 2, Marcel Dekker, New York.
- Giles, C. H., McEwan, T. H., Nakhwa, S. N., and Smith, D. (1960) Studies in adsorption. Part XI. A system of classification of solution adsorption isotherms and its use in diagnosis of adsorption mechanisms and in measurement of specific surface area of solids: *J. Chem. Soc.*, 3973-3993.
- Gregg, S. J. and Sing, K. S. W. (1982) *Adsorption, Surface Area and Porosity*: 2nd ed., Academic Press, Orlando.
- Guerrero-Ruiz, A., Rodríguez-Ramos, I., Fierro, J. L. G., Jiménez-López, A., Olivera-Pastor, P., and Maireles-Torres, P. (1992) Catalytic activity of layered  $\alpha$  (Sn or Zr)-phosphates and chromia pillared derivatives for isopropyl alcohol decomposition: *Appl. Catal.* **92**, 81-92.
- Maireles-Torres, P., Olivera-Pastor, P., Rodríguez-Castellón, E., Jiménez-López, A., and Tomlinson, A. A. G. (1991a) Porous chromia pillared  $\alpha$ -zirconium phosphate materials prepared via colloidal methods: *J. Mat. Chem.* **1**(5), 739-746.
- Maireles-Torres, P., Olivera-Pastor, P., Rodríguez-Castellón, E., Jiménez-López, A., and Tomlinson, A. A. G. (1991b) Porous chromia-pillared  $\alpha$ -tin phosphate materials: *J. Solid State Chem.* **96**, 368-380.
- Mitchell, I. V. (1990) *Pillared Layered Structures, Current Trends and Applications*: Elsevier Applied Science, London.
- Monsted, L., Monsted, O., and Springborg, J. (1985) Evidence for "classical" hydroxo-bridges polymers in hydrolyzed hexaaquachromium: *Inorg. Chem.* **24**, 3496-3498.
- Nakamoto, K. (1986) *Infrared and Raman Spectra of Inorganic and Coordination Compounds*, 4th ed., Wiley, New York.
- Navarro-Martos, J. (1977) *Estudio de la superficie de los geles de  $Al_2O_3$ - $Cr_2O_3$  en función de su composición*: Tesis Doctoral, Universidad de Granada, Spain, 296 pp.
- Pesquera, C., González, F., Benito, I., Mendioroz, S., and Pajares, J. A. (1991) Synthesis and characterization of pillared montmorillonite catalysts: *Appl. Catal.* **69**, 97-104.
- Pinnavaia, T. J., Tzou, M. S., and Landau, S. D. (1985) New chromia pillared clay catalyst: *J. Am. Chem. Soc.* **107**, 4783-4786.
- Poncelet, G. and Schutz, A. (1986) Pillared montmorillonite and beidellite. Acidity and catalytic properties: in *Chemical Reactions in Organic and Inorganic Constrained Systems*, R. Setton, ed., Riedel Publishing Co., Dordrecht.
- Powder Diffraction File (1967) Joint Committee of Powder Diffraction Standards, Philadelphia.
- Stunzi, H. and Marty, W. (1983) Early stage of the hydrolysis of chromium(III) in aqueous solution. I. Characterization of a tetrameric species: *Inorg. Chem.* **22**, 2145-2150.
- Tzou, M. S. and Pinnavaia, T. J. (1988) Chromia pillared clays: in *Pillared Clays: Catalysis Today*, R. Burch, ed., Elsevier, Amsterdam.
- Vaughan, D. E. W. (1988) Pillared clays, a historical perspective: in *Pillared Clays: Catalysis Today*, R. Burch, ed., Elsevier, Amsterdam.

(Received 20 May 1992; accepted 20 January 1993; Ms. 2229)